

A Study on the Corrosion of Stainless Steel (AISI 310) Weldments Deposited on Carbon Steel Plate Aged at 550°C for Different Times

Amany Nagy Kamel

Quality control and quality assurance department, Egyptian nuclear and radiological regulator authority (ENRRA)

ABSTRACT: Corrosion is recognized as a major problem in everyday life. It costs a lot of money every year to control material corrosion; it is of paramount importance that thorough studies and investigations be carried out to estimate how these steel products behave in use. In this respect, their corrosion properties are of paramount importance. The objective of this work is to study of the corrosion behavior of stainless steel (AISI 310) weldments deposited on carbon steel plate aged at 550°C for as weld condition, 50 hr, 500 hr and 1000 hr in 3% NaCl solution, Electrochemical corrosion tests were at room temperature. Results showed that for as weld specimen the corrosion potential is -514 mV.

Anodic polarization curves for aged specimens showed that the current density increases with increasing the applied potential till reaches almost constant value. This can be interpreted to the continuous changes of the surface during the polarization tests. The corrosion current density I_{corr} were in the range of $5.3E-6(A/cm^2)$ to $4.3E-3(A/cm^2)$. The changes in metal structure generally increase its attack by chloride ions. The microstructure of weldment structure was (dendrite structure), it has no major changes after 50 hr aging. The microstructure of carbon steel received materials was ferrite-plus-pearlite microstructure. The microstructure of after aging at 550°C is equi-axed bainite phase surrounding ferrite grains.

Keywords: stainless steel (AISI 310), carbon steel, corrosion, aging

Date of Submission: 06-05-2019

Date of acceptance: 13-05-2019

I. INTRODUCTION

For increasing energy demand nuclear energy is an alternative to overcome the rising fossil fuel pollution and cost; the contribution of nuclear power to total electricity generated by all means is estimated at 10.9% in 2012 [1,2]. The construction of more new nuclear reactors is forecast to increase significantly in coming years once the more efficient, next generations of nuclear reactors, particularly Gen IV, are in the market [3, 4]. The importance targets of new reactor designs fall into four main categories: sustainability, safety and reliability, economics and proliferation resistance and physical protection [5].

Corrosion resistance is one of the most important factors in materials selection for Gen IV supercritical water-cooled reactor (SCWR) concept; It is supposed to be one of the most promising future Generation IV nuclear reactor systems due to its simplified design, compact layout, and high thermal efficiency, comparing with the current state-of-the-art light water reactors (LWRs) [1, 3].

Stainless steels are widely used because of their corrosion resistance; this resistance is rendered by Cr in the alloys (usually 11 wt%) and the formation of a Cr-rich surface oxide layer [6, 7, 8] and it will be one of the most promising candidate materials for making SCWR [4,5]. However, its mechanical strength drops quickly when temperature increases up to 600°C [4]. The maximum fuel cladding hot spot temperature at normal operating conditions of a typical pressure vessel type SCWR with outlet coolant temperature of 500 to 510°C [9,5]. Strengthening is needed if type 310 SS can be applied as material for welding or cladding. Amongst the candidate materials, 310SS stainless steel is deemed very promising.

II. MATERIALS AND ITS PREPARATION METHODS

A carbon steel (CS) sheet with the chemical composition Fe basis - 0.2C- 0.01Cr -0.01Ni-1.37Mn-0.23Si- 0.02S -0.005Mo (wt. %) was used in the present study. Manual shielded metal arc welding (SMAW)

process was used to prepare a deposited carbon steel layers of 310 stainless steel (SS) electrode with chemical composition Fe basis - 0.15C-0.2 Si-2 Mn-25Cr-20Ni (wt. %), classed as AWS (American Welding Society). The electrode diameter $\phi = 4$ mm. Rutile coated shielded arc electrodes were used for depositing weld layer. The deposited layer on the carbon steel sheet with weldment deposited cut into specimens after air cooling.

Some of specimens were subjected to an aging temperature of 550 °C for various holding times 50, 500 and 1000 hr followed by air-cooling. The thermal aging process was performed in a muffle furnace which is automatically controlled with an accuracy of $\pm 5^\circ\text{C}$. An additional Ni-NiCr therm Couple attached to a digital thermal indicator was used to check the temperatures at the furnace throughout the holding time.

The specimens were ground under water on rotating disc, using abrasive paper with grades ranging from 180 to 2000. Then polished to mirrored surface by using diamond paste with grades 3 and 1micron. Metallographic examination was carried out for deposited weldment. The microstructure for as weld conditions and after aging were examined. The deposited stainless steel 310 was electrolytically etched with the condition (10g oxalic acid, 6Vdc, 15-30 s) and Carbon steel was etched with 2% Nital. Specimens were rinsed with alcohol and dried with hot air. The optical microscope (OM) was used for microstructural examination.

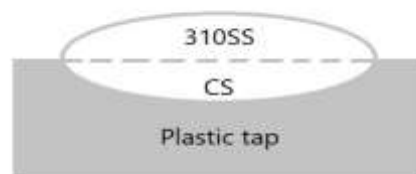
III. EXPERIMENTAL WORK

3-1 Microstructure Examination

The samples for optical microscopic observations were mechanical ground and polished with the standard technique using fine alumina particles and then etched in 5% nital was used for microstructure examination. The microstructures in 310 SS weldment and carbon steels for as weld conditions and after aging were examined.

3-2 Corrosion testing

The electrochemical corrosion behavior of the samples was studied by applying the potentiodynamic polarization technique using a potentiostat (Electrochemical Impedance Analyzer, Model 6310) interfaced to a computer and a three-electrode cell with the sample as a working electrode of exposed area 100 mm², a saturated calomel reference electrode (SCE), carbon electrode as counter electrode. The testing media was 3% NaCl prepared from double distilled water and reagent grade salt. The surface an area of 310SS equal to (carbon steel) CS area which is immersion in the test solution; the rest of CS was covered with plastic tap as show in Figure (1).



Figure(1) The schematic of corrosion sample

The potentiostat described above was operated with potentiodynamic polarization scan technique; with delay time 10 second, initial potential equal -100 mv versus open circuit potential and final potential $+400$ mv versus reference electrode potential and the scan rate was $0.5\text{mV}/\text{sec}$. All electrochemical measurements were measured at room temperature and open to atmosphere.

IV. RESULTS AND DISCUSSIONS

Figure (2) shows the Optical micrograph of the microstructure features of 310SS weldment for as welding condition and after aging. The as welded condition showed that the microstructure consists of austenite (white phase) as a matrix and the ferrite as the second phase (which appears as black phase). The austenite phase consists of cellular-dendritic morphology of grains due to the high cooling rate produced by single pass weld layer. The microstructure of weldment structure (dendrite structure) has no major changes after 50 hr aging, only some carbides at grain boundaries was observed, as shown. With increasing the aging time the ferrite phase network started to dissolve the secondary arms of ferrite phase, for 500 and 1000 hr aged specimens.

In the initial stage of Corrosion of 310SS, Cr is preferentially oxidized by reacting with the inward diffusion of oxygen to form Cr_2O_3 due to its much higher oxygen affinity than Ni and Fe [10]. Meanwhile, outward diffusion of Fe reacts with the oxygen form Fe_3O_4 due to its higher diffusion rate than Ni and Cr [10].

It is well known that stainless steels tend to be sensitized at 500-800°C, resulting in carbide precipitation at grain boundaries [11, 12].

Figure(3) shows the microstructure of carbon steels; the As-received materials and after aging at 550 °C for 50hr, 500 hr and 1000 hr. The as-received materials ferrite-plus-pearlite microstructure as shown in Figure (3-a). The pearlite is distributed uniformly but as irregularly shaped volumes embedded in the ferrite matrix (that is typical of a fine tempered structure) Figure (3-b, c, d) the microstructure of after aging at 550°C. These micrographs show equi-axed bainite phase surrounding ferrite grains. The ferrite grains appear unchanged from those observed in the as-received material. The ferrite phase did not experience any structural change after aging time. The processes of corrosion of carbon steel and the properties of corrosion products are modeled based on a quantitative evaluation of the chemical reactions pertaining to corrosion to elucidate the conditions with which corrosion-protective rust films form [13]. The rust film deteriorates due to the dissolution and shrinkage by aging, and the deteriorated rust film separates the anode and cathode reaction products (Fe_{2+} and OH^- ions) to cause crevice corrosion [13].

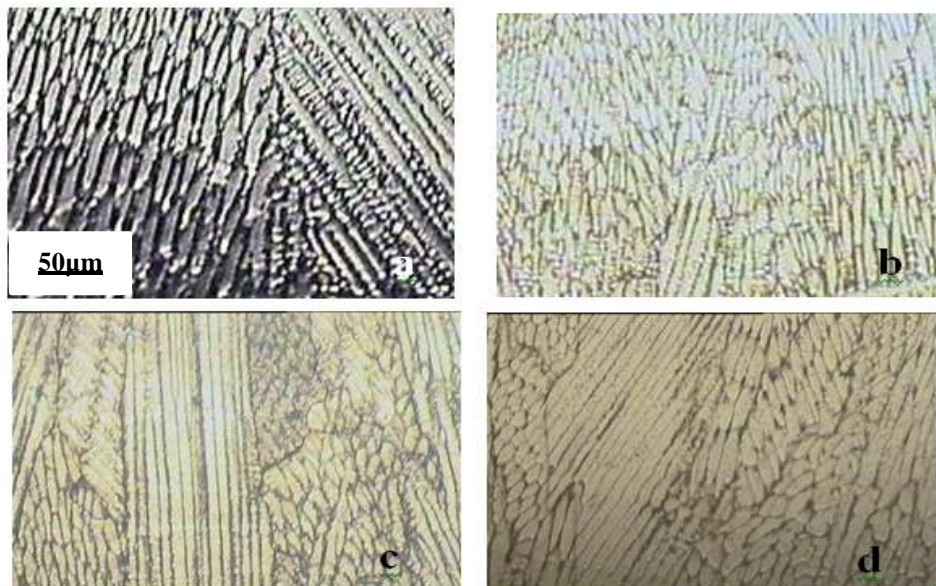


Figure (2) Optical micrograph of the microstructure features of 310SS weldment (a) The As-weld materials (b) 50hr (c) 500hr (d) 1000hr

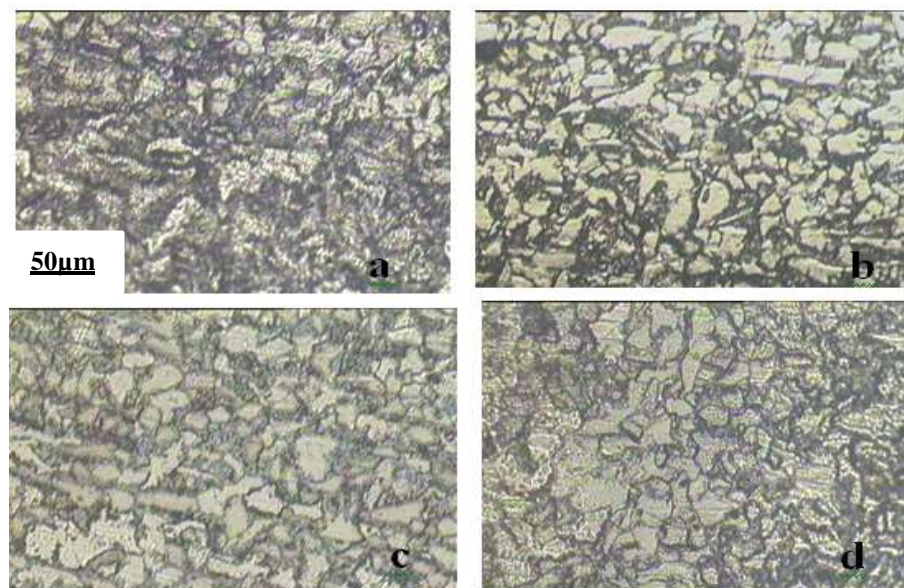


Figure (3) Microstructure of carbon steels (a) The As-received materials (b) 50hr (c) 500hr (d) 1000hr

Anodic polarization curves for specimen(310 SS and CS)for as weld condition in 3% NaCl solution having neutral pH is shown in Figures(4).Anodic polarization curves for aged specimens (310 SS and CS) in 3% NaCl solution are shown in figures (5,7).

In Figure (4) shows the as weld specimen the corrosion potential is -514 mV. The anodic polarization curve shows some irrigators after corrosion potential and the current density increases as potential increases till -380mv, after this potential there is an abrupt increases in current density, which may be due to pits formation then the current density increases till the end of the run.

These figures are of similar behavior but with different values of their electrochemical results. Anodic polarization curves shows that the current density increases with increasing the applied Potential till reaches almost constant value. This can interpreted to the changes on the surface of the alloy.

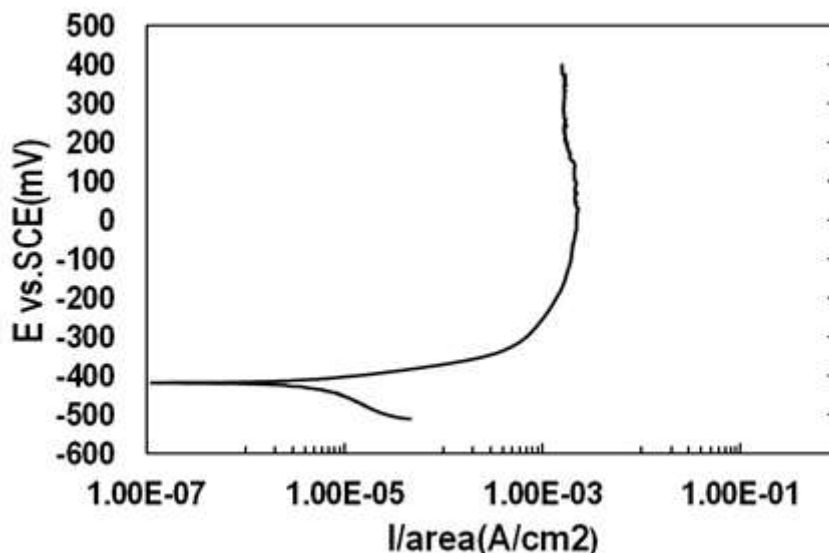


Figure (4) Anodic polarization curve of specimen (310 SS and CS) for as weld condition

The major corrosion type that has been observed for all samples was general corrosion. The corrosion potentials (E_{corr}) of the different conditions of the samples varied in a very narrow range, from -421mV to -522 mV. There were only differences in the corrosion current (I_{corr}) values for the different samples of as weld condition and for aging time.

Figure (5) shows the anodic polarization curve for specimen (310 SS and CS) aging for 50 hr at 550 °C the corrosion potential is -480 mV, the current density increases moderately till -400 mV, after that the current density increases till the end of the run. The corrosion potential is -480 mV which is higher than that of as weld 310SS.

Figure (6) shows the anodic polarization curve for specimen (310 SS and CS) aging for 500 hr at 550 °C, the corrosion potential is- 421mV, in this case the current density increases steadily with content rate to the end of the experiment.

Figure(7) shows the anodic polarization curve for specimen (310 SS and CS) aging for 1000 hr. at 550°C, the corrosion potential is -522 mV ,in this case the current density abrupt increases after corrosion potion with high rate.

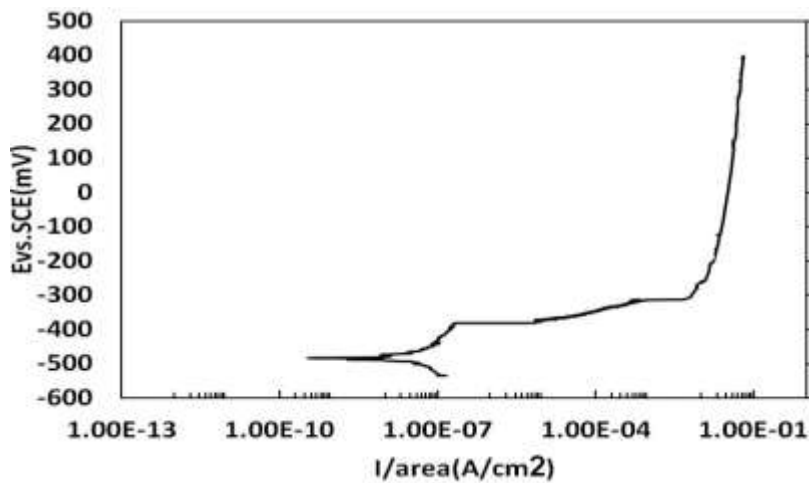


Figure (5) Anodic polarization curve in 3%NaCl solution of sample (310 SS and CS)aging for 50hr at 550°C

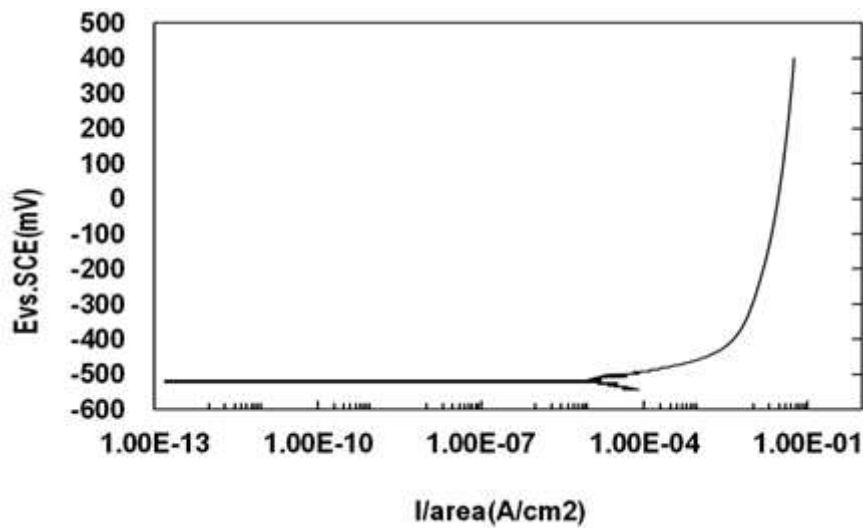


Figure (6) Anodic polarization curve in 3%NaCl solution of sample (310 SS and CS) aging for 500 hr at 550°C

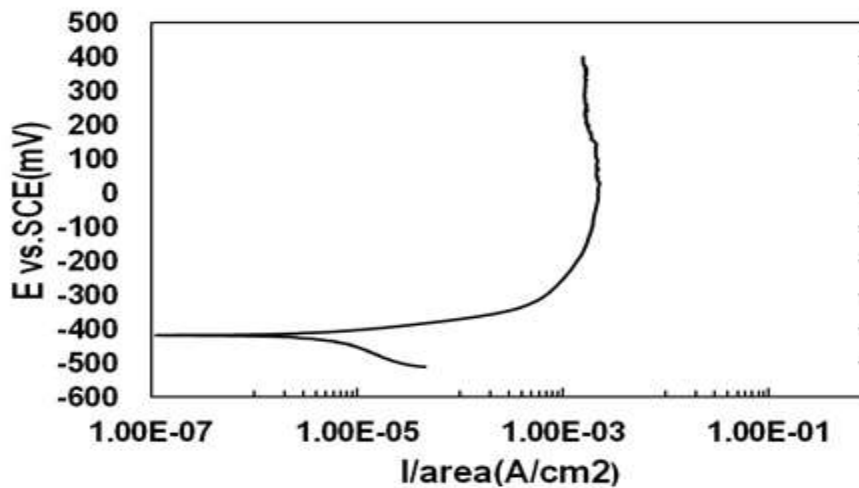


Figure (7)Anodic polarization curve in 3%NaCl solution of sample (310 SS and CS) aging for 1000 hr at 550°C

The corrosion current density I_{corr} and corrosion potential E_{corr} of (310SS) which were determined by potentiodynamic technique are shown in Table (1).

Figure (8) shows the relation between corrosion potential E_{corr} and aging time.

Table(1)Corrosion potential E_{corr} and corrosion current density I_{corr}

| Aging condition | E_{corr} (mV) | I_{corr} (A/cm ²) |
|-----------------|------------------------|--|
| As weld | -514 | 4.3E-3 |
| 50 hr | -480 | 5.3E-6 |
| 500hr | -421 | 300.1E-6 |
| 1000hr | -522 | 1.6E-3 |

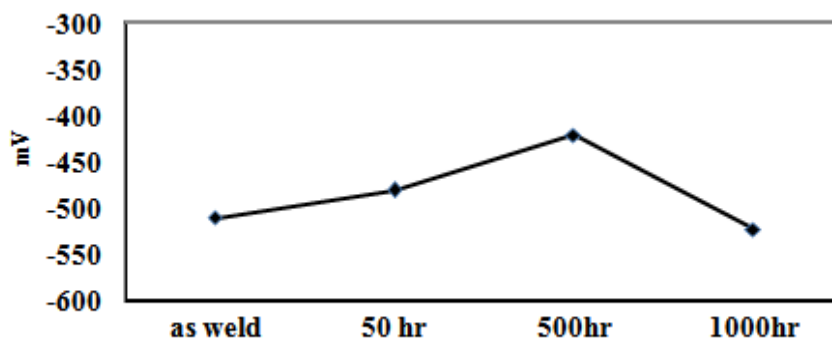


Figure (8) The relation between corrosion potential E_{corr} and aging time hr

The corrosion current densities I_{corr} were in the range of $5.3\text{E-}6(\text{A/cm}^2)$ to $4.3\text{E-}3(\text{A/cm}^2)$. The deformation of metal generally increases its attack by chloride ions. The disarray in the atomic structure is likely to facilitate the detachment of an atom from the metallic phase and its passage into the electrolyte. The energy needed for detachment will surely be less than in the case of an atom occupying a stable position relative to its neighbors. However, the deformation operation presented preferred orientation; therefore there is a chance that these will be liable to suffer rapid attack. The visual notice of the testing solutions during the anodic polarizations of some samples shows a green (GR) suspension. Green rust GR is an intermediate compound between Fe (II) hydroxide and Fe (III) oxyhydroxide and has often been formed by oxidation of $\text{Fe}(\text{OH})_2$ aqueous suspensions. The occurrence of GRs as intermediate compounds in the course of corrosion of iron and steel under aerobic and anaerobic conditions has often been reported [14].

$\text{GR}(\text{Cl-})$ is observed as the main product of the first stage of the corrosion process of the alloy in 3% NaCl solution. The good corrosion resistance after 500h is mainly due to phases formed as shown in Figure (6). The higher Cr content is one of the key factors that contributes to the better corrosion resistance of the supply of Cr and thus may reduce the corrosion rate [15]. The effect of aging on I_{corr} of 310SS is shown in (Table I) for different aging time. This reveals that aging increases the corrosion rate where the deformation twins that created during aging represent regions of different potential from the matrix and this led to the increase in I_{corr} . The temperature limit in oxidizing environments for these materials to maintain their oxidation resistance and mechanical properties can be as high as 1000 °C [16]. In austenitic stainless steels, particularly, the protective surface oxide generally assumes a two- or three-layered structure [17] with magnetite (Fe_3O_4) on the outer surface and an inner layer of oxide with elevated chromium content forming either corundum type $(\text{Cr},\text{M})_2\text{O}_3$ or a spinel type $(\text{Cr},\text{M})_3\text{O}_4$ oxide [18]. Different and versatile corrosion products were found on the carbon steel embedded in the cement mortar after an exposure to wet and dry cycles [13].

V. CONCLUSION

Corrosion is one of the key factors in materials selection. In this paper the study of the corrosion for 310SS weldment deposited on carbon steel plate aged at 550°C for different times have been discussed. The 310SS deposited on carbon exhibits little corrosion resistance in this work, but after the initial 50hr the corrosion current density was less than that of as-weld and other heat treatment temperatures. The microstructure of weldment structure (dendrite structure) has no major changes after 50 hr aging. The microstructure of carbon steels of as-received materials was ferrite-plus-pearlite microstructure. The microstructure of after aging at 550°C is equi-axed bainite phase surrounding ferrite grains.

ACKNOWLEDGEMENT

I wish to express my deep appreciation and sincere gratitude to Prof. Dr.A.F.Waheed metallurgy department. Atomic energy authority, for his help for expermental work ond fruitful discussions and guidance.

REFERENCE

- [1]. Squarer, D., T. Schulenberg, D. Struwe, Y. Oka, D. Bittermann, N. Aksan, Cs Maraczy, R. Kyrki-Rajamäki, A. Souyri, and P. Dumaz. "High performance light water reactor." *Nuclear Engineering and Design* 221, no. 1-3 (2003): 167-180.
- [2]. Kumar, S. Sunil, Neelakantha V. Londe, K. Dilip Kumar, and Md Ibrahim Kittur."A Review on Deterioration of Mechanical Behaviour of High Strength Materials under Corrosive Environment." In *IOP Conference Series: Materials Science and Engineering*, vol. 376,(2018). 1, p. 012106
- [3]. Mayer, K. H., W. Bendick, R. U. Husemann, T. Kern, and R. B. Scarlin. New materials for improving the efficiency of fossil-fired thermal power stations.in: *International Joint Power Generation Conference, PWR*, vol.33, ASME, (1998), p. 831
- [4]. Shen, Zhao, Lefu Zhang, Rui Tang, and Qiang Zhang. "The effect of temperature on the SSRT behavior of austenitic stainless steels in SCW." *Journal of Nuclear Materials* 454, no. 1-3 (2014): 274-282.
- [5]. Zhang, Lefu, Yichen Bao, and Rui Tang. "Selection and corrosion evaluation tests of candidate SCWR fuel cladding materials." *Nuclear Engineering and Design* 249 (2012): 180-187.
- [6]. Shen, Zhao, Kai Chen, Xianglong Guo, and Lefu Zhang. "A study on the corrosion and stress corrosion cracking susceptibility of 310-ODS steel in supercritical water." *Journal of Nuclear Materials* 514 (2019): 56-65.
- [7]. Was, G. S., P. Ampornrat, G. Gupta, S. Teysseyre, E. A. West, T. R. Allen, K. Sridharan et al. "Corrosion and stress corrosion cracking in supercritical water." *Journal of Nuclear Materials* 371, no. 1-3 (2007): 176-201.
- [8]. Monnet, Isabelle, P. Dubuisson, Y. Serruys, Marie-Odile Ruault, O. Kai, and Bernard Jouffrey. "Microstructural investigation of the stability under irradiation of oxide dispersion strengthened ferritic steels." *Journal of Nuclear Materials* 335, no. 3 (2004): 311-321.
- [9]. Naffakh, H., M. Shamanian, and F. Ashrafizadeh."Dissimilar welding of AISI 310 austenitic stainless steel to nickel-based alloy Inconel 657." *Journal of materials processing technology* 209, no. 7 (2009): 3628-3639.
- [10]. Behnamian, Yashar, Amir Mostafaei, Alireza Kohandehghan, Babak Shalchi Amirkhiz, Daniel Serate, Wenyue Zheng, David Guzonas, Markus Chmielus, Weixing Chen, and Jing Li Luo. "Characterization of oxide scales grown on alloy 310S stainless steel after long term exposure to supercritical water at 500 C." *Materials Characterization* 120 (2016): 273-284.
- [11]. Parrens, Coralie, Jacques Lacaze, Benoit Malard, Jean-Luc Dupain, and Dominique Poquillon. "Isothermal and Cyclic Aging of 310S Austenitic Stainless Steel." *Metallurgical and Materials Transactions A* 48, no. 6 (2017): 2834-2843.
- [12]. Dománková, Mária, Edina Kocsisová, Ivan Slatkovský, and Peter Pinke. "The Microstructure Evolution and Its Effect on Corrosion Properties of 18Cr-12Ni-2, 5Mo Steel Annealed at 500-900 C." *Acta Polytech. Hung* 11, no. 3 (2014).
- [13]. BETONA, SIMULIRANI PORNI VODI. "Corrosion properties of different forms of carbon steel in simulated concrete pore water." *Materiali in tehnologije* 48, no. 1 (2014): 51-57.
- [14]. Refait, Ph, O. Benali, M. Abdelmoula, and J-MR Génin. "Formation of 'ferric green rust' and/or ferrihydrite by fast oxidation of iron (II-III) hydroxychloride green rust." *Corrosion science* 45, no. 11 (2003): 2435-2449.
- [15]. Sato, Kazunori, Kazuhiro Tagawa, and Yasunobu Inoue."Modulated structure and magnetic properties of age-hardenable Fe-Mn-Al-C alloys." *Metallurgical Transactions A* 21, no. 1 (1990): 5-11.
- [16]. Kim, Young G., Jae K. Han, and Eun W. Lee."Effect of aluminum content on low temperature tensile properties in cryogenic Fe/Mn/Al/Nb/C steels." *Metallurgical Transactions A* 17, no. 11 (1986): 2097-2098.
- [17]. Charles, J., and A. Berghezan. "Nickel-free austenitic steels for cryogenic applications: The Fe-23% Mn-5% Al-0.2% C alloys." *Cryogenics* 21, no. 5 (1981): 278-280.
- [18]. Ghayad, I. M., N. N. Girgis, W. Ghanem, and A. S. Hamada."Effect of cold working on the aging and corrosion behavior of Fe-Mn-Al stainless steel." (2006).

Amany Nagy Kamel" A Study on the Corrosion of Stainless Steel (AISI 310) Weldments Deposited on Carbon Steel Plate Aged at 550°C for Different Times" *American Journal of Engineering Research (AJER)*, vol.8, no.05, 2019, pp.175-181